J Mater Sci: Mater Med (2012) 23:913–919
DOI 10.1007/s10856-012-4579-5

Synthesis of injectable and cohesive nano hydroxyapatite scaffolds

Nitin Pratap Varma · Subhadra Garai · Arvind Sinha

Received: 27 September 2011 / Accepted: 3 February 2012 / Published online: 16 March 2012
© Springer Science+Business Media, LLC 2012

Abstract Biomimetically synthesized nanosized hydroxyapatite particles have been converted into an injectable paste using a neutral phosphate buffer. Synthesized system manifested a self setting behavior at 37°C in 20 min and revealed a macroporous self assembled microstructure. Stability of the injectable hydroxyapatite has been confirmed in aqueous medium as well as in human blood. Effect of ball milling was also studied on the stability of the system.

1 Introduction

One of the main objectives of tissue engineering in general and bone tissue engineering in particular has been to construct three dimensional porous scaffolds, capable of performing both mechanical and biological functions [1]. Moving ahead from auto grafts, allograft and xenografts based approaches of bone regeneration, the synthetic bone grafts have been now preferred. From the biomaterial science point of view, extensive research has been carried out for the development of synthetic biomaterials, suitable for bone tissue engineering. No doubt, that calcium phosphate (CaP) based bioceramics in general and hydroxyapatite (HA) in particular has been the most applied biomaterial for bone regeneration in its pure form and in a stoichiometric combination with tricalcium phosphate, forming a two phase material, termed as biphasic calcium phosphate (BCP) [2–4]. Recent developments in the field of nanobiomaterials, confirming the stem cell adhesion, proliferation and differentiation on the surface of nanosized HA and BCP particles have revealed the osteoconductive nature of HA and osteoinductive nature of BCP nanoparticles [5–8]. Such findings have brought a paradigm shift from bioinert/biocompatible to bioactive materials based bone treatment. In a simple scaffold based approach of bone void filling, most of the time the extent of the bone void, its location and the function of the damaged bone (load bearing or non load bearing) play a major role in the selection of the scaffold material (osteoconductive or a combination of osteoinductive and osteoconductive) as well as its physical form like powder, granules or three dimensional blocks. However, many times a very narrow bone-damage or bone disintegration, caused by age related pathological fracture, osteoporosis and other related complications, can not be handled with the approaches involving solid scaffolds [9, 10]. To overcome these limitations, minimal invasive procedures are becoming popular in orthopedics and orthodontics [11]. Such a procedure demands an injectable biomaterial equipped with all the necessary structural and functional properties as exhibited by nanosized HA/BCP, along with a self setting property at room temperature. Keeping its three dimensional structure intact under physiological environment, good injectability, non toxicity, an optimum compressive strength and handling time is another set of the required properties of injectable biomaterial for bone regeneration [12–14].

In the recent years, Ca–P based cements (CPC), comprising two or more members of the family of Ca–P mineral as solid component, while a sodium phosphate solution as a cementing liquid have been proposed to be the most suitable biomaterial in the injectable form to deal with narrow and irregular defects of bones [15–18]. Such a two phase system, when injected, leads to the formation of delhite phase during its setting [19]. However, most of these CPC, are known to get disintegrated in presence of water as well as in blood [11, 20, 21].

N. P. Varma · S. Garai · A. Sinha (✉)
CSIR-National Metallurgical Laboratory,
Jamshedpur 831 007, India
e-mail: arvind@nmlindia.org

Overcoming the above limitation of the injectable bone graft, the present manuscript demonstrates and discusses a process to synthesize nano HA based injectable system using biomimetically synthesized HA nanoparticles as a solid phase while a modified sodium phosphate solution as a mixing liquid. It has been interesting to observe that without invoking a typical cement setting reaction, injected nano HA particles, after 20 min incubation at 37°C forms a 3-dimensionally rigid structure, stable under water and blood. A regular necklace like macroporous and stable microstructure of the injected HA, indicates a secondary bonds assisted ordered assembly of HA nanoparticles coated with a neutral phosphate buffer molecules. In this study, a burst phenomenon, rupturing cylinder like injected HA structures in water, was also noticed when HA particles were subjected to a 30 min milling before the injectable cream formation.

It is worth mentioning here that, to the best of our knowledge, the present manuscript may be the first one demonstrating the self setting property of HA nanoparticles. Hence the scope of the study in this report is limited to the synthesis, structural characterization and stability of the injected form in aqueous and biological medium.

2 Experimental

Synthesis of nanocrystalline injectable HA is basically a two step process. First step involves the synthesis of nanocrystalline HA powder characterized by a narrow size distribution and uniform morphology, while second step consists of translating nanocrystalline HA powder into an injectable paste. In the present study, the synthesis of nanocrystalline HA has been carried out by a poly(vinyl alcohol) (PVA) mediated synthesis route, similar to a matrix mediated biomineralization process. This process is termed as biomimetic synthesis and reported in details elsewhere [4, 22–24]. To convert the nanocrystalline HA powder into an injectable form, the HA powder was divided into three groups. Group 1 was used as such for the injectable paste synthesis, while the powders of group 2 and group 3 were subjected to ball milling for 10 and 20 min, respectively. On the other hand a neutral phosphate buffer solution was prepared by mixing mono and di-sodium phosphate solutions of known concentration in a pre-determined volumetric ratio to achieve a neutral pH (pH 7). In three Petri dishes, 2.0 g of nanocrystalline HA powder from each group (group 1, group 2, and group 3) was taken, respectively. All the three HA powders in the Petri dishes were mixed with an optimum volume of neutral phosphate buffer one by one, maintaining a solid/liquid ratio of 1.08 g/ml. Liquid was mixed with the powder using a spatula for 3 min and then transferred into a 3 ml syringe and injected without a needle as well as using a needle of 24 G (within the range as recommended for dental application). Material injected without needle was obtained in the form of long cylinders. It was immediately transferred to an incubator maintained at 35°C and incubated there for 20 min. After incubation all the three samples were immersed in distilled water for the observation of their aqueous stability. All the experiments have been repeated five times for the reproducibility. Samples synthesized under group 1 were designated as N1, while from groups 2 and 3 were N2 and N3, respectively.

Synthesized material was structurally characterized using transmission electron microscopy (TEM CM 200, CX Philips at 160 kV JEOL 2100), X ray diffraction (XRD) (D8 DISCOVER, BRUKER, using Cu–Kα radiation in the degree 2θ range of 10°–80°), scanning electron microscopy (SEM, JEOL 840 A, all the three samples were coated with gold before loading them in SEM), and Fourier transform infra-red spectroscopy (FTIR, 410 JASCO). Structural stability of N1, N2, and N3 was confirmed by immersing their equal weights in equal volume of distilled water and observing the apparent changes in their shape and size, if any. Similarly, sample N1 (weight = 0.05 g) was immersed in freshly extracted human blood (5 ml) and centrifuged at 5,000 rpm for 15 min at room temperature to notice any possible deformation under physiological condition.

3 Results and discussions

The most common limitation of recently developed CPC, comprising one or several of the following components; amorphous calcium phosphate (ACP), dicalcium phosphate dehydrate (DCPD), dicalcium phosphate anhydrous (DCPA), α-tricalcium phosphate (α-TCP), dicalcium phosphate (DCP), tetracalcium phosphate (TTCP), monocalcium phosphate monohydrate (MCPM) and calcium carbonate (CC), has been its structural disintegration under physiological environment [19, 20]. Incorporation of organic molecules, such as sodium alginate, hydroxypropyl methylcellulose, carboxymethyl cellulose, modified starch, glycerol and chitosan to control the washout property of injectable CPC could not address this issue successfully and hence the present study.

Injectable nanocrystalline HA scaffold, synthesized by us and being injected is shown in figures (Fig. 1a, b) exhibiting the injectability with and without the needle. TEM bright field image revealed the size and shape of HA nanoparticles, synthesized by a biomimetic route and used in the synthesis of the three injectable samples (Fig. 2). The XRD pattern of the incubated injectable samples, confirmed the presence of only crystalline HA phase, as

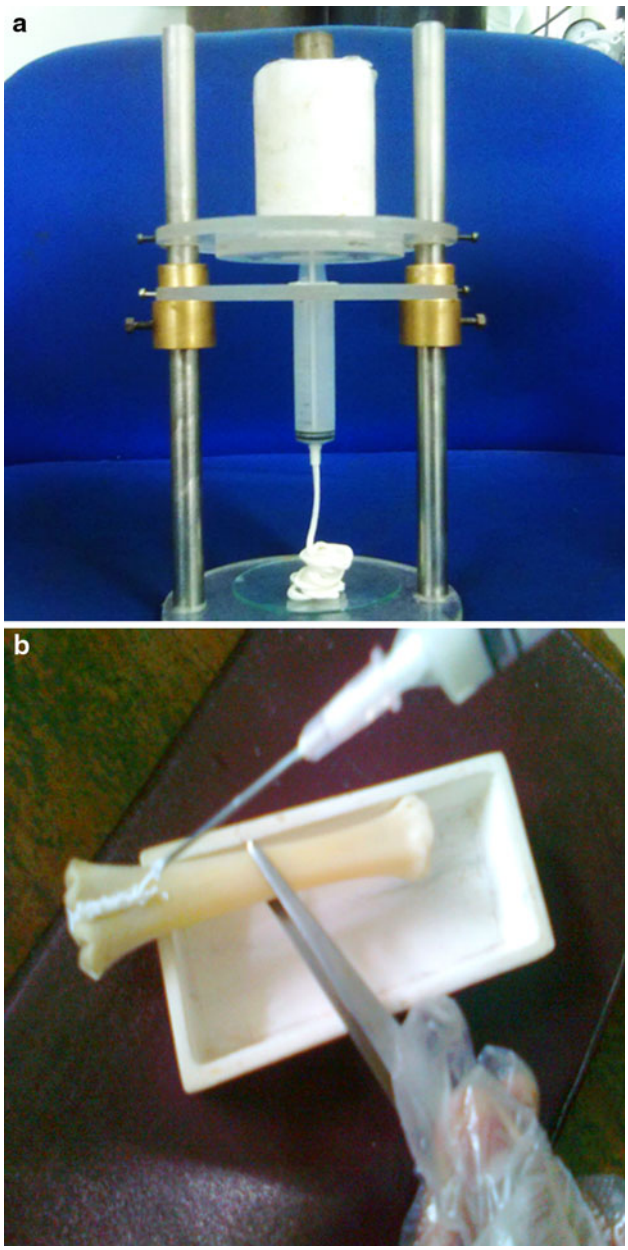

Fig. 1 **a** Injection of nanoHA paste from the syringe without needle. **b** Injection of nanoHA paste from the syringe loaded with 18 gauge needle

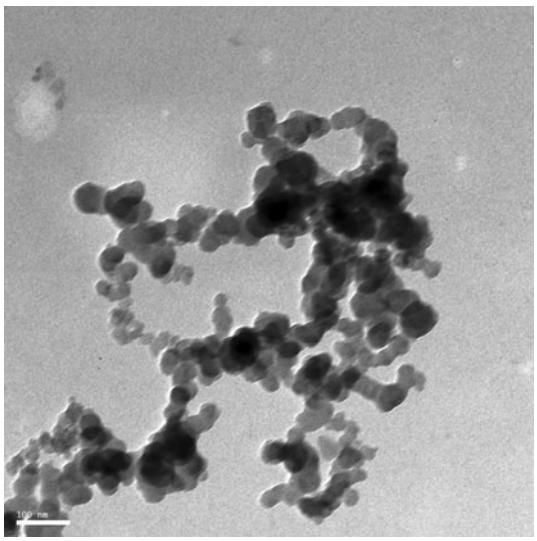

Fig. 2 Bright field TEM micrograph showing shape and size of biomimetically synthesized nano HA particles used for the synthesis of injectable paste

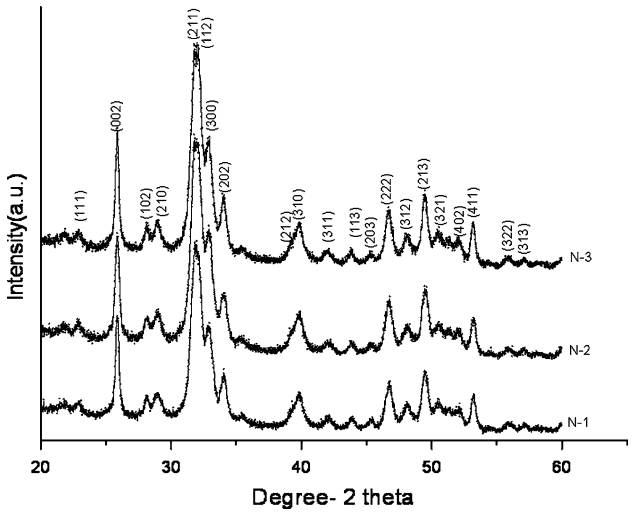

Fig. 3 XRD patterns of sample N1, N2, and N3 after injection and setting, confirming the presence of HA phase only

manifested by (111), (002), (102), (210), (211), (112), (300), (202), (212), (310), (311), (113), (203), (222), (312), (213), (321), (402), (411), (322) and (313) reflections (Fig. 3). A high degree of crystallinity of HA nanoparticles, synthesized at room temperature and exhibiting almost 100% crystalline phase, may be attributed to the biomimetic process of synthesis, where the surface energy associated with the underlying polymer matrix contribute to a good crystallinity of the synthesized material. It is note worthy that all the three samples yielded identical diffraction pattern, except milling induced relative broadening of diffraction peaks, which may be attributed to a combined effect of induced stresses due to defects as well as possible reduction in particle size. Not considering the effect of generated defects due to milling, a calculation of average crystalline size based on well known Scherer's equation (average crystallite size $= K\lambda/\beta{\cdot}\cos\theta$, where K is the constant related with crystallite shape and can be approximated to unity, λ is the wave length of the radiation, β is the peak width in radians at half of the intensity maximum), yielded an average crystalline size of 22.94 nm for sample N1, while 12.51 nm for N2 and 12.06 nm for N3. It is to be mentioned here that milling of HA nanoparticles, on one hand may reduce the average crystallite

size of HA, on the other hand due to presence of moisture and high surface energy of HA nanoparticles, it induces some degree of agglomeration of nanoparticles, leading to an increase of polycrystalline HA particles, due to the well known cementing reaction during ball milling.

SEM microstructures of the three injected samples confirmed the formation of three dimensional porous networks having elongated pore in the size range of 1 to 2 μm (Fig. 4). Injected HA of unmilled material revealed a relatively denser micro structure (Fig. 4a) in comparison to milled ones (Fig. 4b, c). All the three microstructures in general and microstructures of milled samples in particular, manifest a regular networking of HA particles which agglomerated during milling as well as during mixing with sodium buffer and further due to pressure created during injection. Besides the above mentioned harsh environment faced by HA nanoparticles, the regularity in the microstructure observed may be attributed to a mechanism of biomimetic HA setting, which seems to be different from the known mechanism of CPC setting. It is proposed that self setting of CPC takes place due to cementing action of acidic and basic Ca–P compounds on wetting under aqueous atmosphere, leading to the formation of dahllite [19, 25]. However, the stability of CPC under water and physiological conditions could not be ensured [11, 21]. On the other hand, studying the aqueous and physiological stability of the injectable nano HA, we immersed all the three samples (N1, N2, and N3) in distilled water. All the three samples behaved differently, revealing a possible correlation in its microstructure and stability. Figures (Fig. 5a–c) exhibit the state of sample N1 just after immersion in the water (Fig. 5a), after 02 min (Fig. 5b) and after 30 min (Fig. 5c). After that, we have kept this sample in water for over a month and no visible change in its shape and size was observed. However, it was noted that as soon as sample N1 was immersed in water, lots of bubbles were evolving out of the upper surface of the sample, while no bubble formation could be seen from the bottom surface in the Petri dish (Fig. 5a). With time bubble formation was reduced and finally no bubble could be seen after 30 min. Formation of bubbles only from the upper surface of the immersed sample, may be understood in terms of capillary action, caused by the nanosized open pores present across the thickness in the volume of the injected HA. Rising of liquid in these fine pores was responsible for the migration of entrapped air molecules, resulting bubble formation on the top surface of the immersed sample. Bubble formation decreased with time and finally stopped when equilibrium height of water in the capillary was reached. On the contrary, both the injectable samples (N2 and N3), prepared from the ball milled nanocrystalline HA particles, did initially, exhibit bubble formation on its immersion in water, but within 02 min,

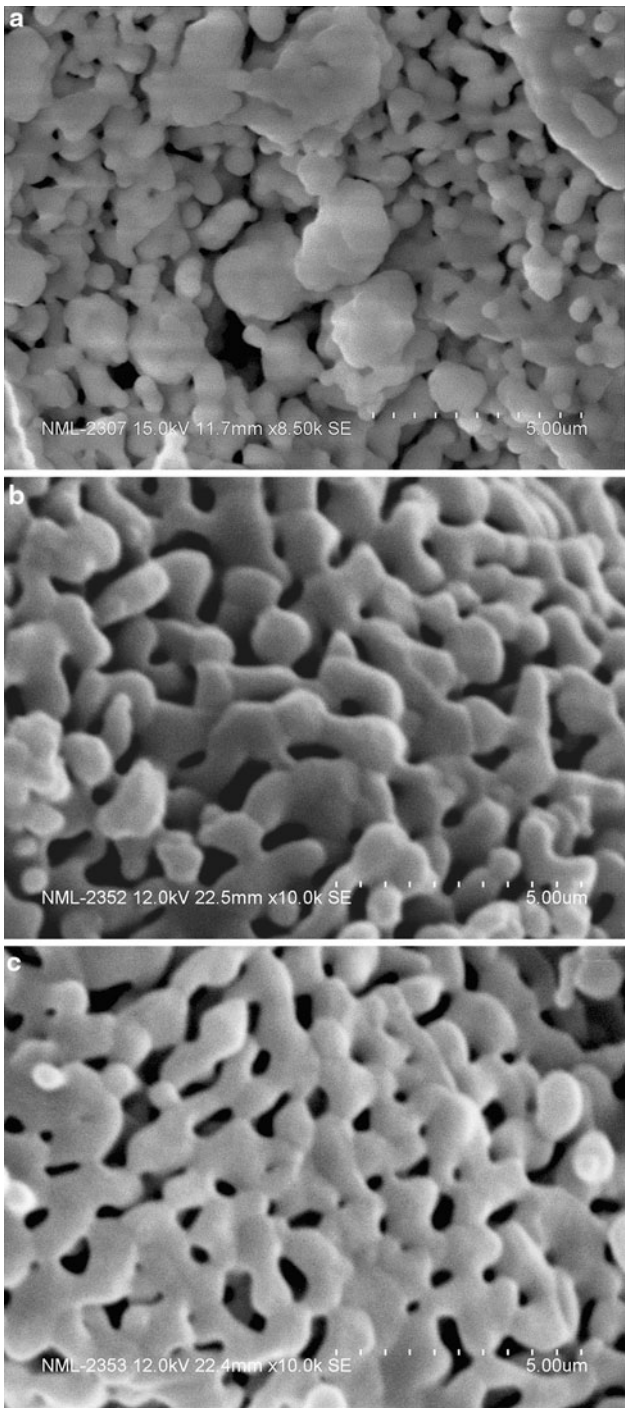

Fig. 4 **a** SEM microstructure of the injected and incubated N1, exhibiting a three dimensional macroporous structure, comprising HA agglomerate in the size range of 0.5–2.5 μm. **b** SEM microstructure of the injected and incubated N2, exhibiting a three dimensional macroporous structure, comprising an ordered pattern looks to be resulted from a self assembly like process. **c** SEM microstructure of the injected and incubated N3, exhibiting a three dimensional macroporous structure, comprising an ordered pattern looks to be resulted from a self assembly like process

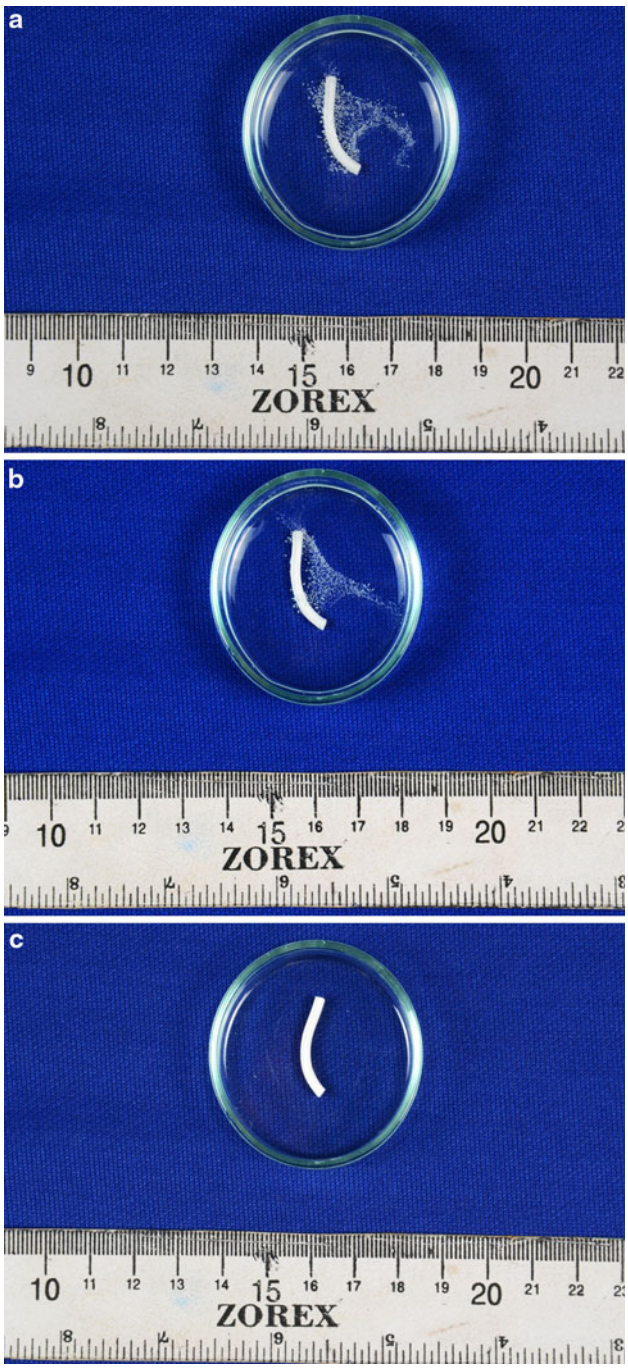

Fig. 5 **a** Sample N1, just after immersion in distilled water, exhibiting bubble formation from the top surface of the sample immersed. **b** Sample N1 after 2 min of immersion in the water revealing a reduction in rate of bubble formation. **c** Sample N1 after 30 min of immersion in distilled water exhibiting no bubbles at all and a totally intact sample in the water

both were burst and ruptured into smaller pieces (Fig. 6a, b). Ruptured pieces were relatively finer in the size in case of N3 rather than N2. It is worth mentioning here that after the rupture of N2 and N3, no more decomposition or dissolution of the broken pieces could be seen, even after a

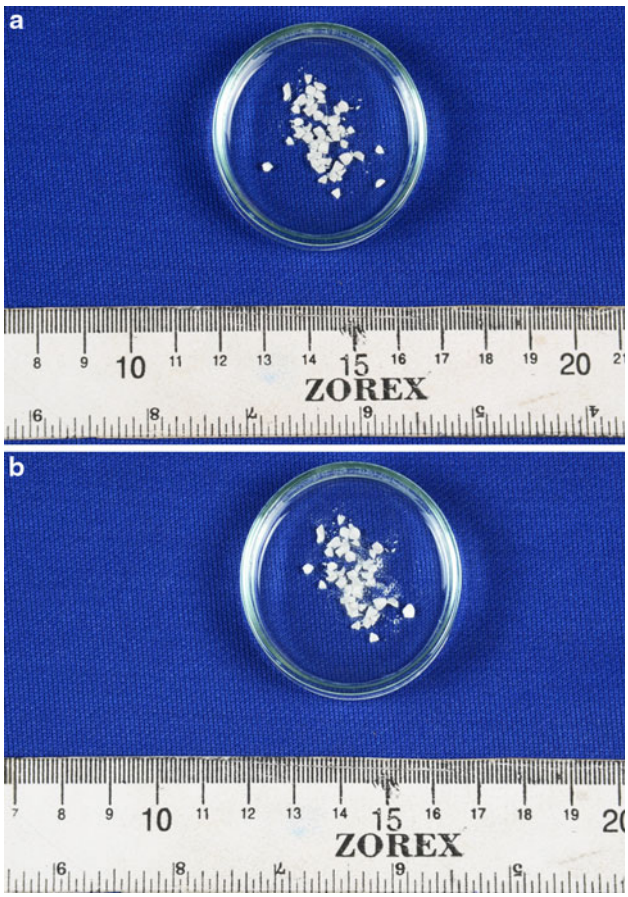

Fig. 6 **a** Sample N2, after 2 min of immersion in distilled water, showing ruptured sample. **b** Sample N3, after 2 min of immersion in distilled water, showing ruptured sample

month of continuous immersion in water, confirming the failure to be a purely mechanical in nature and not dependent on the chemistry of the material. Rupture of N2 and N3 may be attributed to sudden expansion and compression of air bubbles during its transport along the capillary having variable cross section along its length. However, injectable sample N1 seems to be having capillaries of uniform cross sectional area, hence the high stress generated in case of N2 and N3 due to the sudden compression and expansion was not the case with N1. In order to ensure the stability of the synthesized material in blood, we have dipped the injected nano HA rods of sample N1 (as only N1 was found stable under aqueous environment) in freshly extracted human blood and then centrifuged it at 5,000 rpm for 15 min, we could not notice any deformity in the material (Fig. 7a, b).

Chemical characterization of the three samples using FTIR revealed almost similar absorption spectra (Fig. 8). All the recorded absorption bands are tabulated and indexed in the table (Table 1). Along with characteristic –OH, P–O and P–O–P band of HA, –CH2 and –CH bands

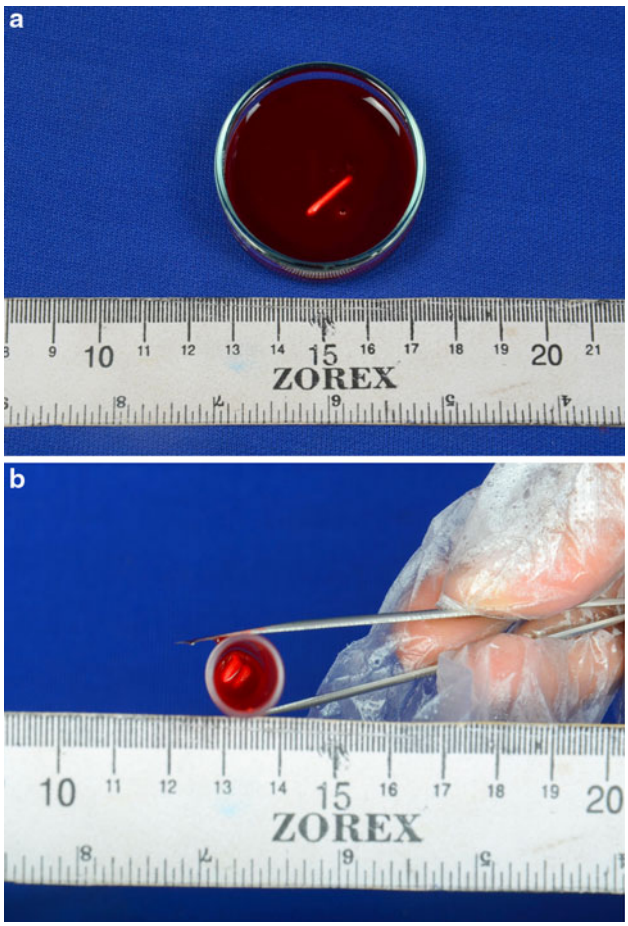

Fig. 7 **a** Sample N1 after 15 min immersion in human blood, revealing an intact injected structure. **b** Sample N1 after 15 min of immersion in human blood followed by a centrifuge at 5,000 rpm for 5 min, showing undamaged injected structure

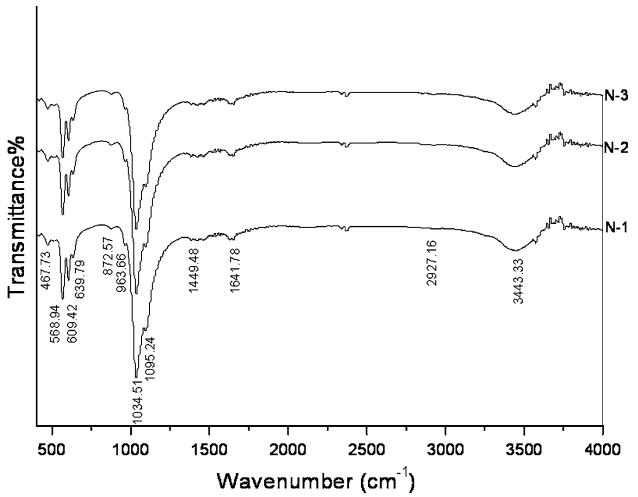

Fig. 8 FTIR spectrum of N1, N2, and N3 revealing no effect of milling over the chemical structure of the samples

Table 1 Absorbance bands of different groups present in samples

S. No	Wave number (cm^{-1})	Assigned
1	467.73	P–O–P (stretching)
2	568.94	P–O–P (stretching)
3	609.42	
4	639.79	
5	872.57	HPO_4^{-2}
6	963.66	P–O (stretching)
7	1034.51	
8	1449.48	$–CH_2$ (stretching)
9	1641.78	–OH (bending)
10	2927.16	CH (stretching)
11	3443.33	OH (stretching)

of PVA were also observed confirming the presence of PVA in the synthesized HA system. Possibly, the presence of available hydrogen bonds, due to in situ HA precipitation in the PVA matrix, as described in our earlier references [22–24], may be correlated with the secondary bonds, steric entrapment, and in turn self assembly assisted cementing of HA nanoparticles on injection [26]. Presently, it is a proposition only and needs further confirmation.

In summary, the present manuscript reports the synthesis of injectable nano HA system, making use of biomimetically synthesized HA nanoparticles and a modified sodium phosphate buffer. A high stability of the injectable system in water and as well as in human blood makes it an attractive system for the injectable scaffolds for bone regeneration. In comparison to commonly available CPC powders, involving multi phosphates of calcium, the present study demonstrates a single phase based injectable material, again simplifying the synthesis and the cost of the product.

It is well known that a complete characterization of an injectable product requires the optimization of solid: liquid ratio used in the synthesis, and its effect on structure–property correlations, handling time before the injection, injectability, mechanical properties under compression and in vivo and in vitro response. Most of these studies are on and will be reported separately as the main focus of the present communication is limited to the possibly first report on the synthesis of self setting and injectable nano HA system.

4 Conclusions

A process has been developed to convert biomimetically synthesized nano HA into injectable and self setting HA scaffolds, without involving the conventional ingredients of bone cement. In comparison to aqueous instability of commonly available CPC systems, in the present

communication, the nano HA based system has established its stability in both water as well as in human blood. An interesting phenomenon of self setting behavior of HA nanoparticles at neutral pH, makes them distinct from CPC setting mechanism dependent on acidic and basic components of CaPs involved. The setting behavior of nano HA based system may be attributed to a combined effect of H-bond cross linking of PVA molecules and physical entrapment in addition to well known cementing action of the phosphate buffer.

Acknowledgments Authors acknowledge the financial support received from CSIR network project under XI Five Year Plan (NWP 0051) and also from M/S IFGL Refractory, Kolkata.

References

1. Langer R, Vacanti JP. Tissue engineering. Science. 1993;260: 920–6.
2. Hutmacher DW, Schantz JT, Lam CXF, Tan KC, Lim TC. State of the at and future directions of scaffold based bone engineering from a biomaterials perspective. J Tissue Eng Regen Med. 2007; 1:245–60.
3. Habraken W, Wolke JGC, Jansen JA. Ceramic composites as matrices and scaffolds for drug delivery in tissue engineering. Adv Drug Deliv Rev. 2007;59:234–48.
4. Guha AK, Singh S, Kumaresan R, nayar S, Sinha A. Mesenchymal cell response to nanosized biphasic calcium phosphate nanocomposites. Colloids Surf B 2009; 73:146–151.
5. Webster TJ, Ergun C, Doremus RH, Siegel RW, Bizios R. Enhanced function of osteoclast like cells on nanophase ceramics. Biomaterials. 2001;22:1327–33.
6. Webster TJ, Siegel RW, Bizios R. Enhanced function of osteoblast on nanophase ceramics. Biomaterials. 2000;21:1803–10.
7. Sujatha G, Sinha A, Singh S. Cells behaviour in presence of nano-scaffolds. J Biomed Nanotech. 2011;7:43–4.
8. Habibovic P, de Groot K. Osteoinductive biomaterials-properties and relevance in bone repair. J Tissue Eng Regen Med. 2007;1: 25–32.
9. Youssef JA, Salas VM, Loshiavo RG. Management of painful osteoporotic vertebral fractures: vertebroplasty and kyphoplasty. Oper Tech Ortho. 2003;13:222–6.
10. Bohner M, Lemaitre J, Cordey J, Gogolewski S, Ring TA, Perren SM. Potential use of biodegradable bone cement in bone surgery: holding strength of screws in reinforced osteoporotic bone. Orthopaedic Trans. 1992;16:401–2.
11. Yu T, Ye J, Wang Y. Synthesis and property of a novel calcium phosphate cement. J Biomed Mater Res B. 2009;90:745–51.
12. Philips FM. Minimally invasive treatments of osteoporotic vertebral compression fractures. Spine. 2003;28:S45–53.
13. Heini PF, Berlemann U. Bone substitutes in vertebroplasty. Eur Spine J. 2001;10:S205–13.
14. Bohner M, Baroud G. Injectability of calcium phosphate pastes. Biomaterials. 2005;26:1553–63.
15. Fernandez E, Gill FJ, Ginebra MP, Driessens FCM, Planell JA, Best SM. Calcium phosphate bone cements for clinical applications. Part I: solution chemistry. J Mater Sci Mater Med 1999; 10:169–176.
16. Brown WE, Chow LC. Dental restorative cement pastes. US patent No. 4 518 430, 1985, American Dental Association Health.
17. Bai B, Jazrawi LM, Kummer FJ, Spivak JM. The use of an injectable, biodegradable calcium phosphate bone substitute for the prophylactic augmentation of osteoporotic vertebrae and the management of vertebral compression fractures. Spine. 1999;24: 1521–6.
18. Bohner M, Lemaitre J, Ring TA. Effects of sulfate, pyrophosphate and citrate ions on the physicochemical properties of cements made of beta-tricalcium phosphate-phosphoric acid water mixtures. J Am Ceram Soc. 1996;79:1427–34.
19. Hou Q, De Bank PA, Shakesheff KM. Injectable scaffold for tissue regeneration. J Mater Chem. 2004;14:1915–23.
20. Komath M, Varma HK, Sivakumar R. On the development of an apatitic bone cement. Bull Mater Sci. 2000;23:135–40.
21. Komath M, Varma HK. Development of a fully injectable calcium phosphate cement for orthopedic and dental applications. Bull Mater Sci. 2003;26:415–22.
22. Sinha A, Nayar S, Agrawal A, Bhattacharya D, Ramachandrarao P. Synthesis of nanosized and microporous precipitated hydroxyapatite in synthetic and biopolymers. J Am Ceram Soc. 2003;86: 357–60.
23. Nayar S, Sinha A. Systematic evolution of a porous hydroxyapatite-poly(vinyl alcohol)–gelatin composite. Colloids Surf B. 2004;35:29–32.
24. Sinha A, Mishra T, Ravishanker N. Polymer mediated synthesis of hydroxyapatite microsphere for drug delivery. J Mater Sci Mater Med. 2008;19:2008–11.
25. Chow LC, Takagi S. A natural bone cement—a laboratory novelty led to the development of revolutionary new biomaterials. J Res Nat Inst Stand Technol. 2001;106:1029–33.
26. Bohner M, Doebelin N, Baroud G. Theoretical and experimental approach to test the cohesion of calcium phosphate pastes. Eur Cells Mater. 2006;12:26–35.